Global NEST Journal, Vol 25, No 1, pp 115-126

Effects of ultraviolet radiation on the community structure and metabolic pathways of A^{2}O process in plateau environment

Zong Y*., Wang J., He Q., Guo M., You J. and Zhang D.
Water Conservancy Project & Civil Engineering College, Tibet Agriculture & Animal Husbandry University, Linzhi Tibet 860000, China
Received: 01/07/2022, Accepted: 27/10/2022, Available online: 22/11/2022
*to whom all correspondence should be addressed: e-mail: zyc_2001@sohu.com
https://doi.org/10.30955/gnj.004390

Graphical abstract

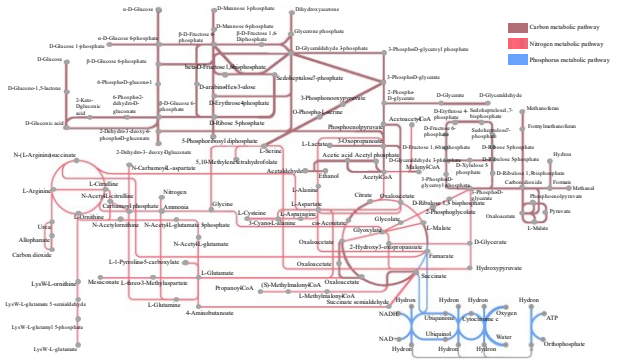

Abstract

Water treatment ecosystems provide an important habitat for a variety of bacterial communities, but the mechanisms by which this ecosystem responds to UV irradiation are unclear. For this reason, 16S rRNA gene sequencing was used to study bacterial community structure and metabolic pathways under UV irradiation. It was shown that bacterial communities were different under different UV irradiation, suggesting that the time of UV irradiation has an effect on the structure of bacterial communities. Analysis of the drivers showed that COD, pH, TN and NH_3-N also had an effect on the relative abundance of keystone species. The key species under UV irradiation were *Bacteroidetes*, *Proteobacteria*, *Actinobacteria*, *Firmicutes*, *Chloroflexi*, and *Chlamydiae*, accounting for 96.69% to 98.30%, and UV irradiation had a significant inhibitory effect on the relative abundance of key species. *Chlamydiae*, as the dominant bacterial phylum in the highland environment, was identified for the first time. Network co-occurrence plots constructed under different UV radiation showed that each sample consisted of three independent network plots. There are six common dominant phyla and 33 common dominant bacterial genera in each sample, which reveals that the ecosystem is structured by more similar microorganisms rather than a random phenomenon. This also reflects the competitive relationships between species and the adaptability of bacteria to their environment. The analysis of metabolic pathways revealed that the dominant metabolic pathways in the highland environment changed somewhat under UV irradiation. Further analysis of carbon, nitrogen and phosphorus metabolic pathways showed that there were some changes in the relative abundance of the relevant metabolic pathways, but the differences in the metabolic maps were minimal, i.e., the effects of UV radiation were mainly reflected in the relative abundance of the metabolic pathways. These findings suggest that UV radiation in the plateau environment acts as an important influencing factor on the structure and metabolic pathways of microorganisms. This study provides an important theoretical basis for further understanding of the water treatment ecosystem in the plateau environment, and also provides a new perspective for the study of wastewater treatment systems.

Keywords: Plateau environment, ultraviolet radiation, community structure, metabolic pathway, A^{2}O

1. Background

Tibet is located in the southwestern of the Qinghai-Tibet Plateau, with an average elevation of more than 4000 meters (Zong *et al.*, 2019), and is known as the roof of the world. High altitude creates unique habitat conditions of high cold, low air pressure and strong ultraviolet rays (UV), which have a greater impact on the operation of sewage treatment, which is manifested by poor nitrogen and phosphorus removal effects and even sewage treatment that cannot meet the sewage discharge standards (Zong *et al.*, 2020; Li *et al.*, 2021).

UV rays are the main component of solar radiation, and there is a positive correlation between the two (Gelsor *et al.*, 2019). Studies have shown that the UV radiation of Lhasa at an altitude of 3,600 meters is more than 1.5 times that of other cities in China, and the plateau is a strong UV radiation area (Zong, 2017). At present, UV rays is often used for disinfection after sewage treatment, and it has an inactivating effect on bacteria, especially when the UV wavelength is 280-320nm, the sterilization effect is the most significant. The disinfection effect of UV rays depends on the effective radiation dose to microorganisms and the resistance of microorganisms to UV rays (Yang *et al.*, 2019). The latest theory shows that activated sludge is a collection of many microorganisms, and that have a large difference

in UV sensitivity (Hughes *et al.*, 2005), and an appropriate amount of UV radiation will change the construction of microorganisms. Wei (2012) uses UV lamps to simulate the irradiation of sewage treatment processes (The energy of UV radiation is 30.91J). Short-term irradiation (40s) can increase the removal rates of COD, TP, and TN by 5.83%, 2.16%, and 19.51%, respectively. But when the UV radiation is 60-80s, the removal rate of pollutants is reduced (Wei, 2012; Jiang *et al.*, 2003) used UV radiation (20W ultraviolet germicidal lamp radiation for 0.5min), which can increase the rate of TP removal of activated sludge by 4%～8%, but when the radiation time exceeds 3min, the TP removal rate is significant decline. Hao (2021) have tested and found that UV radiation has a certain effect on the removal rate. The increased content of G^+ and N^+ bacteria in activated sludge after irradiation is an important reason for the enhancement of its phosphorus removal performance. UV rays do not mutagenize bacteria by radiation, but kill or inhibit the nutrient competition of phosphorus removal bacteria in activated sludge-non-phosphorus accumulating flora, providing an optimized environment for rapid growth of phosphorus removal bacteria and enhance Phosphorus removal performance of activated sludge. The study of (Zhao *et al.*, 2005) found that after 3 minutes of 15W of UV lamp irradiation at a distance of 20cm from the activated sludge, the most significant change in the activated sludge microbial group was *β-Proteobacteria*, with a lethality rate of more than 90%, and the smallest change was *γ- Proteobacteria*, and the survival rate became 81.89%, and the *α-proteobacteria* group became 20.75% of the original, and the survival rates of *Pseudomonas* and *Commonas* are 40.31% and 41.16%, respectively, which indicates that the sensitivity of various groups in activated sludge to UV ray is quite different. However, longer-time UV exposure will cause the total microbial biomass in activated sludge to decrease (Monyethabeng *et al.*, 2016).

The A^2O process is a mainstream biological treatment process for water treatment plants in Tibet (Zong *et al.*, 2018). The A^2O process has a simple operating principle, low construction cost, easy management, and simultaneous nitrogen and phosphorus removal, which is the biggest advantage of the A2O process. Therefore, many scholars have conducted pilot tests of the A2O process at high altitude in Tibet to investigate the effects of temperature (Hao *et al.*, 2021), hydraulic retention time (HRT) (You *et al.*, 2022) and dissolved oxygen (DO) (Yuanwei *et al.*, 2021) on the effluent quality as well as microbial community structure.At present, there is no direct study on the changes of metabolic pathways in sewage treatment under UV radiation, but related studies on plants have shown that UV radiation can change genes and affect metabolic pathways. Zhou (2020) found UV-C irradiation promoted the synthesis of phenols, flavonoids and anthocyanins by up-regulating expressions of phenylalanine ammonia-lyase e, 4-coumarate-CoA ligase, chalcone synthase, dihydroflavonol 4-reductase and UDP-glucose: flavonoid glucosyltransferase when transcriptomics and proteomics approaches were applied to investigate changes in peaches treated with UV-C. Dewen (2020) found 1,826 up-regulated and 1,872 down-regulated genes in the research of leaf responses and differentially expressed genes of Eucommia ulmoides Oliver for transcriptome profiling after ultraviolet-B radiation (UV-B) in the east-north China. And among them, the up-regulated unigenes were mainly participated in Signal transduction mechanisms, and Cell wall/membrane biogenesis by the KOG database, and up-regulated genes were analyzed in plant hormone signal transduction and phenylpropanoid metabolic pathways by KEGG pathway.

The above analysis shows that UV radiation has a certain effect on the community structure and metabolic pathways of sewage treatment. Therefore, revealing the law of microbial composition and metabolic pathways changes in the A^2O process under different UV is to explore the microbes and metabolism under UV in Plateau environment. The need for pathway response mechanism is also one of the most important theoretical foundations in exploring the mechanism of water treatment system affected by Plateau environment. Therefore, this study selects the A^2O system as a typical sewage treatment process to carry out the experimental research under UV, using SPSS20.00, starting from the community structure and metabolic pathway response, discussing the experimental rules corresponding to UV changes, and analyze and reveal the response mechanism of community structure and metabolic pathways in A^2O process.

2. Materials and Methods

2.1. Test device

A laboratory-scale A^2O system is used in experimental research (Figure. 1). The main control parameters are that the effective volume is 210L, and it is divided into 3 compartments, which are anaerobic tank, anoxic tank and aerobic tank. The volume ratio is 1:1:2.5, and the volume of the sedimentation tank is 39L. The stirring device is set at the bottom of the anaerobic tank and the anoxic tank, the stirring speed is 50 rpm, and an aeration head is provided at the bottom of the aerobic tank to supply oxygen. Peristaltic pumps are used to control the water inflow, return sludge and nitrification liquid. In the test, a thermostatic circulator is used to control the water temperature, and each tank wall is equipped with sampling ports.

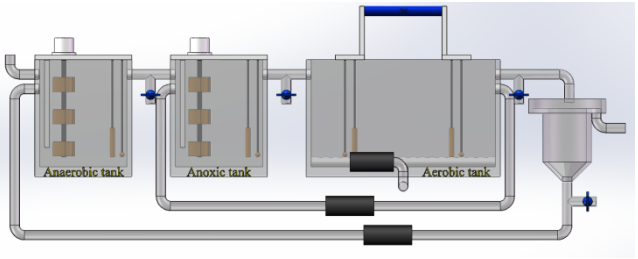

Figure 1. A^2O process device.

Activated sludge was domesticated at 20.0℃ for 35 da ys, SV_{30} was 35%, and MLSS was 4178mg/L. The domestic sewage in Nyingchi City is used as the test water. The specific operating parameters are that the designed influent flow rate is 10.0±0.1L/s, the dissolved oxygen of

the aerobic tank is controlled to 2 mg/L, the hydraulic retention time is 21.0±0.2h, and the anaerobic tank retention time: Anoxic tank residence time: the aerobic tank residence time is 1:1:2.5, the mixed liquid reflux ratio is R_i=200%, the sludge reflux ratio is R=100%, the mixed liquid and sludge are continuously refluxed to dissolve. The oxygen change is achieved by blast aeration, and the temperature is controlled at 20°C. UV is realized by 40w UV lamp. The irradiation time is 0min (blank group), 5min, 10min, 30min, 180min, and the distance is 20cm. The water quality sampling is 72h after the irradiation change.

2.2. UV radiation setting

In this experiment, the activated sludge surface area of 0.053 m2 in the aerobic tank was irradiated with a length of 53 cm and a power of 40w UV lamp at a distance of 20 cm from the sludge surface for 0, 5, 10, 30 and 180 min. The radiation intensity was simulated using UV power and irradiation distance, and the calculation formula was as follows.

$$S = \frac{P}{2\pi\gamma L},$$

(P indicates the UV power, γ indicates the irradiation distance, and L indicates the length of the UV lamp), then S ($1m^2 \cdot s$) = 60.05J. Thus, the irradiation times of 0, 5, 10, 30 and 180 min correspond to radiation intensities of 0, 954.80, 1909.59, 5728.77 and 34372.62 J, respectively.

2.3. 16S rRNA gene sequencing

Samples for this experiment were entrusted to Shanghai Meiji Biomedical Technology Co., Ltd. for testing (htpp://www.majorbio.com). The 16S rRNA sequencing started with DNA extraction using 1% agarose gel electrophoresis and PCR primers 338F (ACTCCTACGGGAGGCAGCA) and 806R (GGACTACHVG-GGTW TCTAA T) were amplified in variable region V3-V4 and initial sequence quality screening was performed. Duplicate data (100% similarity clustering) removal operation was performed using the DADA2 method (Callahan *et al.*, 2016). Finally, species annotation was performed on the QIIME2 cloud platform based on the Silva database (Release 132, http://www.arbsilva.de) (Quast *et al.*, 2012).

2.4. Statistical methods of data

In this paper, non-metric multidimensional scaling (NMDS) analysis was performed using the software Qiime to calculate the beta diversity distance matrix, and the R language vegan package for NMDS analysis and graphing (version 3.3.1). The Kruskal-Wallis rank sum test (Kruskal-Wallis H test) was used for the analysis of species differences between groups. This analysis allows the analysis of significant differences between species in multiple sample groups. Correlation heatmap plots were made using the software R (version 3.3.1) (pheatmap package), by calculating the correlation coefficients between environmental factors and selected species (Spearman rank correlation coefficient, Pearson correlation coefficient, etc.), and the obtained numerical matrix was visualized through Heatmap plot. The Network analysis step generates clusters based on the species shared among the samples, and there are two types of nodes (nodes) in the network graph, a species-node and a sample-node. Diagram of carbon, nitrogen and phosphorus metabolism was plotted with the help of KEGG database, and the relative abundance of each metabolic pathway was constructed by combining PICRUSt2 functional prediction and Origin 2021.

3. Results and discussion

3.1. Bacterial diversity and community composition under different irradiation time

In total, 642,049 high-quality sequences and 12812 OTUs were obtained through 16S rRNA high-throughput sequencing. The richness index of OTUs in all samples was 1314. Among them, there were 418 OTUs in all samples, accounting for 31.84% of the total number of OTUs. There were 734 OTUs in uv_0, accounting for 55.86% of the total number of OTUs. There were 745 OTUs in uv_5, accounting for 56.70% of the total number of OTUs. There were 835 OTUs in uv_10, accounting for 63.55% of the total number of OTUs. There were 802 OTUs in uv_30, accounting for 61.04% of the total number of OTUs. There were 890 OTUs in uv_180, accounting for 67.73% of the total number of OTUs. The community richness sobs indexes of the five samples are 561, 627, 637, 594, and 649. Obviously, only some of the OTUs in the five samples are the same. At the same time, comparing the OTUs and sobs indexes of uv_0 with the other four samples, it can be shown that UV radiation will increase the types of microorganisms. The similarity analysis of NMDS and ANOSIM in Figure 2 showed that the bacterial community composition among the five samples was significantly different (R=0.5778, P≤0.001).

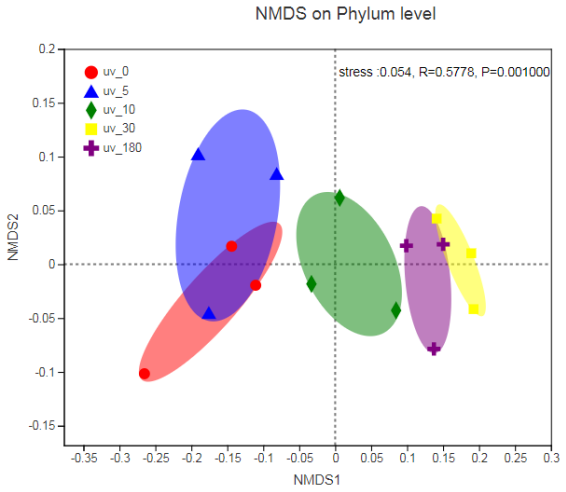

Figure 2. Non-metric multidimensional scale (NMDS) of bacterial community composition.

The differences of the five samples at phylum level and genus level are shown in Figures 3 and 4, respectively. The key species at the phylum level are *Bacteroidetes*, *Proteobacteria*, *Actinobacteria*, *Firmicutes*, *Chloroflexi*, and *Chlamydiae* in Figure 3. The relative abundances of the above bacterial phyla are 98.30%, 97.57%, 96.69%, 97.45%, 97.02% in five samples. UV radiation has a certain inhibitory effect on the relative abundance of the above-mentioned dominant bacteria phyla as a whole, and the

inhibitory effect of 10 minutes of radiation is the largest. The relative abundances of *Bacteroidetes* were 12.90%, 16.56%, 30.00%, 42.87% and 37.11%, respectively, that is, UV radiation has a strengthening effect on *Bacteroidetes*, and its strengthening effect is the largest when the irradiation time is 30min, which is 2.32 times more than uv_0.The relative abundances of *Proteobacteria* were 32.53%, 24.24%, 22.94%, 23.68%, and 27.68%, respectively, that is, UV radiation has an inhibitory effect on *Proteobacteria*, and its inhibitory effect is the largest when the radiation time is 10 minutes, which is 9.58% less than uv_0. The relative abundances of *Actinobacteria* were 32.24%, 31.37%, 24.39%, 19.23%, and 19.61%, which means that UV radiation has an inhibitory effect on *Actinobacteria*, and the inhibitory effect is the largest when the irradiation time is 30 minutes, which is up to 13.00% less than the uv_0. The relative abundances of *Firmicutes* were 15.65%, 19.82%, 13.98%, 8.59%, and 9.22%, namely, it has a strengthening effect when short-term UV radiation (5min) and long-term UV radiation has an inhibitory effect. When the irradiation time is 30min, it inhibits the greatest effect. The relative abundances of *Chloroflexi* were 3.83%, 4.20%, 4.22%, 2.64%, and 2.66%. The abundance shows that short-term UV radiation (within 10min) has a certain strengthening effect while long-term UV radiation (above 30min) will show inhibition. The relative abundances of *Chlamydiae* were 1.15%, 1.38%, 1.17%, 0.44%, and 0.73%, respectively. *Chlamydiae* and *Chloroflexi* under UV rays showed the same trend. In addition, *Chlamydiae* has not been recorded as a dominant bacteria phylum in the ecosystem of wastewater treatment in the existing literature, and it may be a special dominant bacteria phylum in Plateau environment.

The key species at the genus level are *norank_f__AKYH767*, *norank_f__Saprospiraceae*, *Acineto-bacter*, *IMCC26207*, *Candidatus_Microthrix*, *Gordonia*, *Ottowia*, *Trichococcus*, *Comamonas* in Figure 4. The relative abundance of the above bacterial genera in the five samples were 48.75%, 39.96%, 43.50%, 52.50%, 45.52%, that is, except when the irradiation time is 30 minutes, UV radiation has a certain inhibitory effect on the relative abundance of the above-mentioned dominant bacteria. The inhibitory effect of the 5-minute irradiation time is the most obvious. *Acinetobacter* is a phosphorus-polymerizing bacterium that is useful for phosphorus removal (Merzouki *et al.*, 1999). *Ottowia* uses biodegradable organic matter for the denitrification of nitrite (Wang *et al.*, 2018). *Trichococcus* reported as dominant hetero-trophic denitrifying bacteria in oligotrophic niche (Peng *et al.*, 2018). *Comamonas* has a potential role in biofilm-mediated denitrification in aerobic biological processes (Wu *et al.*, 2015). The relative abundances of *norank_f__AKYH767*, *norank_f__Saprospiraceae*, and *Ottowia* show an increasing trend under UV rays, that is, UV irradiation has a strengthening effect on the above-mentioned bacterial genus, and the UV irradiation time corresponding to the maximum abundance is 30min, 30min and 180min, respectively. The relative abundance of *Acinetobacter*, *IMCC26207*, *Candidatus_Microthrix*, *Gordonia*, and *Commonas* showed a decreasing trend under UV radiation, that is, UV has an inhibitory effect on the above bacterial genera. The UV radiation time corresponding to the minimum abundance is 180min, 30min, 30 min, 180 min and 180 min, the relative abundance of *Acinetobacter* and *Gordonia* was significantly different in the five samples ($P<0.05$). The relative abundance of *Trichococcus* showed a trend of being strengthened under short-term UV irradiation (5min), and showed a trend of being suppressed under long-term UV irradiation, but its relative abundance was significantly different among the five samples ($P < 0.05$).

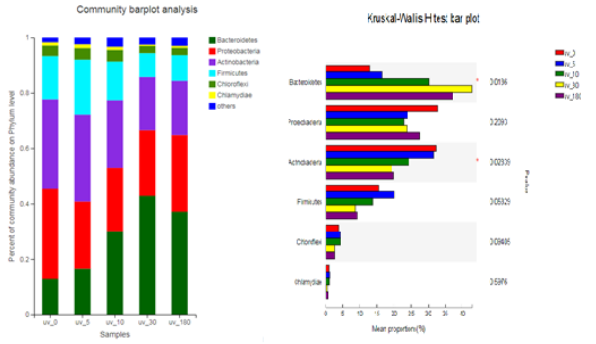

Figure 3. The relative abundance and difference of bacterial communities among samples at the phylum.

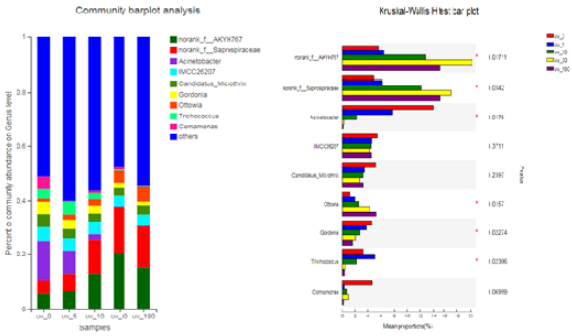

Figure 4. The relative abundance and difference of bacterial communities among samples at the genus.

Through the analysis of the bacterial diversity and community composition in the five samples, it can be found that UV radiation can change the bacterial diversity and community composition, but the key species at the phylum and genus level have not changed. Only the relative abundance of the corresponding key species is changed, and the effect of UV rays is mainly reflected in the two aspects of inhibition and enhancement. However, *Chlamydiae* has a higher relative abundance compared with other regions, and is a unique dominant bacteria phylum in Plateau environment.

3.2. Driving factor analysis

Correlation analysis was carried out on water quality (TN, TP, COD, NH_3-N, BOD_5), environmental factors (such as pH, temperature, DO, UV, etc.) and the richness index of the five samples, and it was found that only the COD and the Shannon showed a significant positive correlation

(r=0.9170, P<0.05). The above-mentioned water quality and environmental factors did not explain the changes in bacterial communities very well. PCA was used to remove noise and redundancy on five samples, and dimensionality reduction analysis showed that UV, COD, and pH had a significant (P<0.05) influence on it, but its interpretation was only 56.05%.

In view of the low interpretation of the samples by the above indicators, water quality indicators and environmental factors are used to further study the impact of key species at the phylum and genus level. The analysis results are shown in Figure 5. At the phylum level, the phyla that are significantly related to temperature, DO and NH_3-N do not exist. The phyla that are significantly related to UV are *Bacteroidetes* (r=0.7965, p<0.001), *Actinobacteria* (r=-0.87287, p<0.001), *Firmicutes* (r=-0.74194, p<0.01), *Chloroflexi* (r=-0.6001, p<0.05), the phyla that are significantly related to pH are *Bacteroidetes* (r=0.56658, p<0.05), and the phyla that are significantly related to COD are *Firmicutes* (r=0.62192, p<0.05), *Chloroflexi* (r=0.57828, p<0.05), the phyla that are significantly related to TN are *Proteobacteria* (r=0.56737, p<0.05), *Actinobacteria* (r=0.54554, p<0.05), The phyla that are significantly related to NH_3-N are *Proteobacteria* (r=-0.56737, p<0.05), *Actinobacteria* (r=-0.54554, p<0.05), and the phyla that are significantly related to BOD_5 are *Chloroflexi* (r=0.53806, p<0.05). The negative and significant correlation between pH (pH>7) and *Bacteroidetes* is contrary to the conclusion of the literature (pH<7) (Hou *et al.*, 2020), which may be related to the neutral pH of *Bacteroidetes*. The relative abundance of *Proteobacteria*, which are nitrogen-fixing bacteria, and *Actinobacteria*, which are denitrification bacteria, are positively correlated with TN. However, biological nitrogen fixation will reduce nitrogen to NH_3-N, that is, when NH_3-N is high, it will reduce the nitrogen fixation reaction rate and decrease the abundance of corresponding bacteria such as *Proteobacteria* and *Actinobacteria*. *Chloroflexi* (Xian *et al.*, 2020) is positively related to BOD_5 as a bacterium that removes organic and removes sulfur.

At the genera level, the genera that are significantly related to DO and TP do not exist. The genera that are significantly related to UV are *norank_f__AKYH767* (r=0.72012, p<0.01), *norank_f__Saprospiraceae* (r=0.73103, p<0.01), *Acinetobacter* (r=- 0.91652, p<0.001), *IMCC26207* (r=-0.53463, p<0.05), *Candidatus_Microthrix* (r=-0.53463, p<0.05), *Gordonia* (r=-0.93834, p<0.001), *Ottowia* (r=0.94925, p <0.001), *Trichococcus* (r=-0.76376, p<0.001), *Propioniciclava* (r=-0.77467, p<0.001), *unclassified_f__Propionibacteriaceae*(r=-0.64374, p<0.01), *Romboutsia* (r=-0.70921, p<0.01), *Dietzia* (r=-0.7965, p<0.001), *Novosphingobium* (r=0.61156, p<0.05), *Clostridium_sensu_stricto_13* (r=-0.88378, p<0.001). The genus significantly related to DO is *norank_f__Saprospiraceae* (r=0.52689, p<0.05), which may be related to the genus (Li *et al.*, 2019) as aerobic phosphorus removal bacteria. The genus that is significantly related to temperature is *norank_f__Saprospiraceae* (r=0.55556, p<0.05), which is a bacterium that is easily inhibited by low temperature (Zong *et al.*, 2019). The genera that are significantly related to pH are *norank_f__AKYH767* (r=0.55585, p<0.05), *norank_f__Saprospiraceae* (r=0.65416, p<0.01), *Gordonia* (r=-0.6059, p<0.05), *Novosphingobium* (r=0.53667, p<0.05), where *norank_f__Saprospiraceae* is consistent with the description in the literature (Gao *et al.*, 2020). Because the most suitable condition for *Gordonia* is pH 7.0 (Yan *et al.*, 2015), it is inversely proportional to pH. The genera that are significantly related to COD are *Trichococcus* (r=0.62192, p<0.05), *Romboutsia* (r=0.63283, p<0.05) (Xia *et al.*, 2018), *unclassified_f__Propionibacteriaceae* (r=0.72012, p<0.01), *Christensenellaceae_R-7_group* (r=0.67648, p<0.01), most of the above-mentioned bacteria are those that degrade organic. The genera significantly related to TN are *IMCC26207* (r=0.67648, p<0.01), *Gordonia* (r=0.52372, p<0.05), and the genera significantly relate to NH_3-N is *IMCC26207* (r=-0.67648, p <0.01), *Gordonia* (r=-0.52372, p<0.05), the genus significantly relate to BOD_5 are *unclassified_f__Propionibacteriaceae* (r=0.57016, p<0.05), *Christensenellaceae_R-7_group* (r=0.64001, p<0.05), analysis shows that UV, temperature, pH, COD, TN, NH_3-N and BOD_5 are indicators that have an impact on dominant bacterial genera.

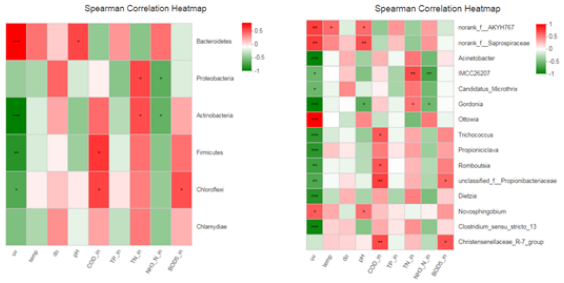

Figure 5. Correlation analysis of key species and environmental factors at the phylum and genus level.

The analysis of environmental driving factors shows that the quality and environmental factors have no significant impact on the diversity and composition of samples, but UV, COD, pH, TN and NH_3-N have a greater impact on the relative abundance of dominant bacteria.

Network co-occurrence under different irradiation times

In order to further reveal the formation mechanism of differences among the five samples, 50 dominant genera are used to construct species coexistence relationships under 5 samples. The parameters are set as spearman (r≥0.5) for correlation coefficient and p<0.05 for significance coefficient. The network analysis diagram is shown in Figure 6. The results show that under the set parameters, five samples form a disconnected network diagram, and the network diagram of each sample is composed of three independent network diagrams. The sample of uv_0 is composed of 49 genera of six phyla including *Proteobacteria*, *Actinobacteria*, *Bacteroidetes*, *Chloroflexi*, *Firmicutes*, and *Chlamydiae*, forming three independent network diagrams of 21, 18, and 10 nodes respectively. The sample of uv_5 is composed of 50 genera of seven phyla including *Proteobacteria*, *Actinobacteria*, *Bacteroidetes*, *Patescibacteria*, *Chloroflexi*, *Firmicutes*, and *Chlamydiae*, forming three independent network diagrams

with 17, 17, and 16 nodes respectively. The sample of uv_10 is composed of 50 genera of eight phyla including *Actinobacteria*, *Patescibacteria*, *Proteobacteria*, *Bacteroidetes*, *Chloroflexi*, *Firmicutes*, *Chlamydiae*, *Epsilonbacteraeota*, forming three independent network diagrams of 28, 15, and 7 nodes, respectively. The sample of uv_30 is composed of 50 genera of six phyla including *Proteobacteria*, *Actinobacteria*, *Bacteroidetes*, *Chloroflexi*, *Firmicutes*, and *Chlamydiae*, forming three independent network diagrams of 23, 15, and 12 nodes respectively. The sample of uv_180 is composed of 50 genera of seven phyla including *Proteobacteria*, *Actinobacteria*, *Bacteroidetes*, *Patescibacteria*, *Chloroflexi*, *Firmicutes*, and *Chlamydiae*, forming three independent network maps of 22, 14, and 14 nodes, respectively. A total of 71 genera appeared in the network, of which 33 genera were shared by five samples. The 4 genera are the dominant genera with irradiation time within 30min, namely *unclassified_f__Intrasporangiaceae*, *Turicibacter*, *Meso-rhizobium*, *Clostridium_sensu_stricto_13*. *Norank_f__AKYG1722* is a new dominant genus after UV irradiation. The 5 genera are newly added dominant genera after UV irradiation for more than 10 minutes, namely *unclassified_f__Sphingomonadaceae*, *Rhodo-bacter*, *norank_f__Propionibacteriaceae*, *Chlorobium*, and *Acetoanaero-bium*. *Acinetobacter* and *norank_f__TC1* are the dominant genus of irradiation time within 10min. Others 4 genera are the dominant genera with irradiation time of more than 30min, namely *Taibaiella*, *Roseomonas*, *Proteocatella*, and *norank_f__Hydrogenophilaceae*. Four dominant genera that exist within 5 min of irradiation time, namely *Raineyella*, *Microbacterium*, *Chryseobac-terium*, and *Bosea*. Four dominant genera with only 0min irradiation time are *Exiguobacterium*, *Psychrobacter*, *Pseudomonas*, *Rubellimicrobium*. Four dominant genera with only 180 min irradiation time are *Thaurea*, *OLB17*, *norank_f__SC-I-84*, *Desulfobulbus*, *Alicycliphilus*. The co-occurrence anal-ysis of single factors at the phylum and genus level shows that UV radiation can change the com-position of domi-nant bacteria. Some dominant bac-teria are strengthened or inhibited by UV radiation, and some dominant bacteria are closely related to the length of UV radiation. The above results verify that the sensitivity of microorganisms to uv is quite different (Hughes *et al.*, 2005).

The single-factor network co-occurrence analysis of the microbial community shows that three independent network structures are formed in five samples. The number and composition of these structures depend on the UV radiation time. It further reveals that the structure of the ecosystem is composed of more similar microorganisms, rather than random phenomena (Zhang *et al.*, 2021). Taking into account the similarity and genetic relationship of niche, the microorganisms in the structure may still have a competitive relationship. Six common dominant phyla and 33 common dominant bacterial genera in different samples shows stability. It reflects the competitive relationship and adaptability to the environment.

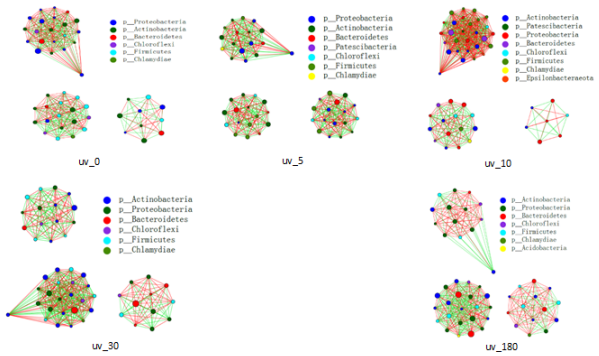

Figure 6. Network co-occurrence under different irradiation time.

3.3. Metabolic pathways under different irradiation time

The changes in the top 20 dominant metabolic pathways in relative abundance under different irradiation times are shown in Figure 7. Among them, the relative abundance increases under UV radiation are Metabolic pathways (map01100), Biosynthesis of secondary metabolites (map01110), Biosynthesis of amino acids (map01230), Carbon metabolism (map01200), Ribosome (map03010), Purine metabolism (map00620)), Glycolysis / Gluconeogenesis (map00010), Carbon fixation pathways in prokaryotes (map00720), Pyrimidine metabolism (map00240), Glycine, serine and threonine metabolism (map 00260), Aminoacyl-tRNA biosynthesis (map00970), that is, the above metabolic pathways are all intensified by UV radiation. The relative abundance reduced under UV rays are Microbial metabolism in diverse environments (map01120), ABC transporters (map02010), Two-component system (map 02020), Glyoxylate and dicarboxylate metabolism (map00630), Fatty acid metabolism (map01212), Valine, leucine and isoleucine degradation (map00280), that is, the above-mentioned metabolic pathways are all inhibited by UV radiation.

With reference to the carbon metabolism diagram, carbon metabolism pathways include Glycolysis/Gluconeogenesis (map00010), Citrate cycle (TCA cycle, map00020), Pentose phosphate pathway (map00030), Methane metabolism (map00680), Carbon fixation in photosynthetic organisms (map00710), Carbon fixation pathways in Prokaryotes (map00720). The relative abundance of the above metabolic pathways is shown in Figure 8. It can be seen from Figure 8 that the T test shows that the above metabolic pathways are all significantly different($p < 0.05$). The relative abundance of Glycolysis / Gluconeogenesis (0.975%～1.025%) is enhanced under UV radiation, but its strengthening gradually weakens as the irradiation time increases. The TCA cycle (0.693% ～ 0.777%) and the Pentose phosphate pathway (0.544% ～ 0.599%) are strengthened under UV irradiation, and the Methane metabolism (0.685% ～ 0.715%) is strengthened under 5min irradiation but over 5min irradiation Inhibited, Carbon fixation in photosynthetic organisms (0.381% ～ 0.459%) and Carbon fixation pathways in prokaryotes (0.945%～0.990%) are strengthened under UV radiation.

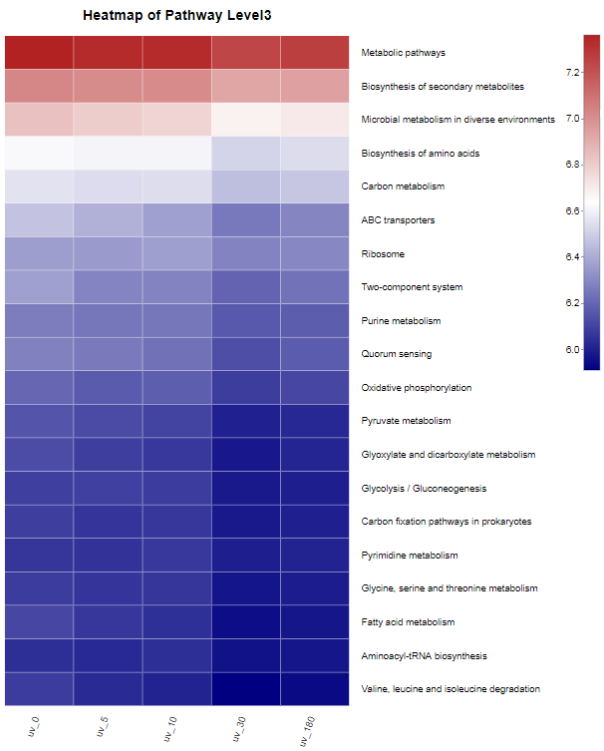

Figure 7. Heat map of the top 20 metabolic pathways of five samples.

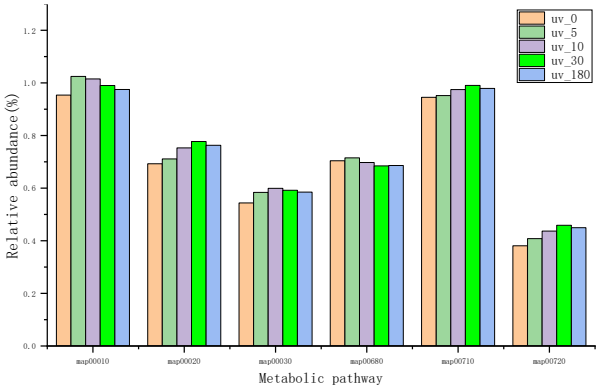

Figure 8. Carbon metabolism pathways of five samples.

Refer to the nitrogen metabolism diagram, the carbon and nitrogen pathways include Alanine, aspartate and glutamate metabolism (map00250), Arginine biosynthesis (map00220), Cyanoamino acid metabolism (map00460), Glyoxylate and dicarboxylate metabolism (map00630), Nitrogen metabolism (map00910). The relative abundance of pathways is shown in Figure 9. It can be seen from Figure 9 that the T test shows that the above metabolic pathways are all significantly different($p < 0.05$). The relative abundance of Arginine biosynthesis (0.452% ～ 0.459%), Alanine, aspartate and glutamate metabolism (0.963%～ 0.990%) is enhanced by UV radiation except 180 minutes, Glyoxylate and Dicarboxylate metabolism (0.782% ～ 0.807%) and Nitrogen metabolism (0.705%～0.723%) are inhibited under UV irradiation except for 30 minutes, and Cyanoamino acid metabolism (0.251% ～ 0.279%) is strengthened under UV irradiation.

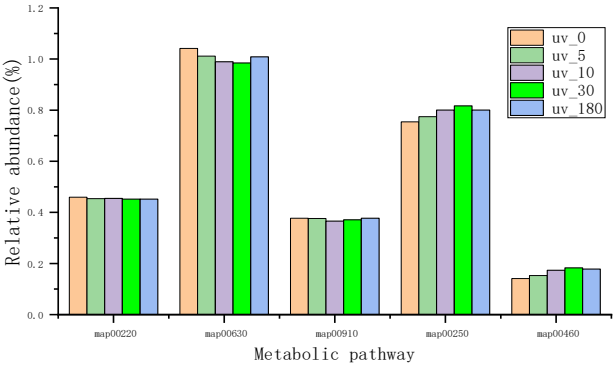

Figure 9. Nitrogen metabolism pathways of five samples.

With reference to the existing literature (Hao *et al.*, 2021), the phosphorus metabolism pathway mainly includes Oxidative phosphorylation (map00190) and Pentose phosphate pathway (map00030). The Pentose phosphate pathway (map00030) participates in both carbon metabolism and phosphorus metabolism, so it is no longer to analyze its metabolic pathway, only Oxidative phosphorylation (map00190) is analyzed, and its relative abundance is shown in Figure 10. It can be seen from Figure 10 that the T test shows that Oxidative phosphorylation (1.287% ～ 1.289%) presents a significant difference($p < 0.05$), and its relative abundance is enhanced by UV irradiation except for 5 min.

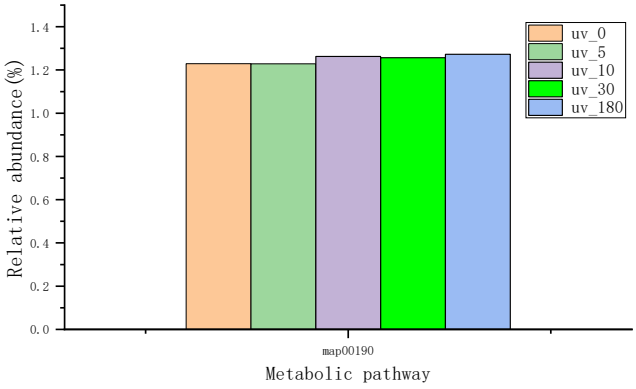

Figure 10. Phosphorus metabolism pathways of five samples.

Refer to the metabolic diagram and use the extracted functional genes to draw the metabolic diagram of carbon, nitrogen, and phosphorus. The main metabolic pathways include Glycolysis/Gluconeogenesis (map00010), Citrate cycle (TCA cycle, map00020), Pentose phosphate pathway (map00030), Methane metabolism (map00680)), Carbon fixation in photosynthetic organisms (map00710), Carbon fixation pathways in prokaryotes (map00720), Alanine, aspartate and glutamate metabolism (map00250), Arginine biosynthesis (map00220), Cyanoamino acid metabolism (map00460), Glyoxylate and dicarboxylate metabolism (map00630), Nitrogen metabolism (map00910), Oxidative phosphorylation (map00190), the results of the drawing are shown in Figure 11.

In the carbon metabolism pathway, the metabolism diagram of Glycolysis/Gluconeogenesis (map00010) in the five samples is exactly the same. The metabolic pathway involved in 2,3-Bisphospho-D-glycerate does not form a

pathway, and it does not exist in five samples. The metabolic diagram formed by the TCA cycle (map00020) in five samples are exactly the same, and their metabolic diagram are complete. The metabolic diagrams of the five samples of the Pentose phosphate pathway (map00030) are completely consistent, and the metabolic pathways involved in D-arabino-Hex-3-ulose 6-phosphate and 2-Dehydro-3-deoxy-D-gluconate did not form a pathway, and both were absent in the 5 samples. In Methane metabolism (map00680), only Coenzyme F420 biosynthesis forms a complete metabolic pathway, while Coenzyme M biosynthesis, Coenzyme B biosynthesis, and Methanofuran biosynthesis do not form an effective pathway. The enzymes and genes corresponding to the above three reactions are almost 0. Metabolic pathways of five samples are exactly the same. In the metabolic pathways of Carbon fixation in photosynthetic organisms (map00710), the metabolic pathways involved in Pyuvate, Alanine, Sedoheptulose and Aspartate did not form pathways, and the metabolic pathways corresponding to five samples were completely the same. The metabolic diagram of Carbon fixation pathways in prokaryotes (map00720) are not completely consistent, and there is no 4-Hydroxybutyryl-CoA, 4-Hydroxybutanoic acid, Succinate semialdehyde, 3-Hydroxypropanoate, 3-Hydro-xypropionyl-CoA, Propenoyl-CoA, 3-Oxopropanoate, (3S)-Citryl-CoA in five samples. In addition, the metabolic pathways of Crotonoyl-CoA and (S)-3-Hydroxybutanoyl-CoA did not form effective pathways in the samples UV_0, UV_10, UV_30, and UV_180. This may be related to the strengthening effect of UV rays on EC: 4.2.1.17 and EC: 1.1.1.35 (the corresponding functional groups are K15016) only when the irradiation time is 5 minutes. The sum of the relative abundances of the 6 carbon metabolism pathways in five samples were 8.660%, 9.147%, 9.301%, 9.330%, and 9.240%. The absolute abundances of the carbon metabolism pathways all showed a decreasing trend except for the uv_5 sample. The formation of carbon metabolism diagram in Plateau environment is incomplete, and the absolute abundance of carbon meta-bolic pathways shows a downward trend under the action of UV rays. Among the six metabolic pathways, except for Carbon fixation pathways in prokaryotes (map00720), the metabolic pathways are almost the same, and UV rays mainly affect Abundance of carbon metabolic pathways.

In the nitrogen metabolism pathway, N-Acetyl-L-aspartate, N-Acetylaspartylglutamate, N-Acetyl-aspartyl-glutamylglutamate, 2-Oxosuccinamate did not form an effective pathway in the metabolic pathways of Alanine, aspartate and glutamate metabolism (map00250) in five samples, and the metabolic diagram is complete. Arginine biosynthesis (map00220) has formed a complete meta-bolic diagram in five samples, and the five samples are exactly the same. Cyanoamino acid metabolism (map00460) forms a poor metabolic diagram, mainly due to the absence of most of its functional genes and enzymes, which may be related to the plateau environment. In the metabolic pathway of Glyoxylate and dicarboxylate metabolism (map00630), Dihydroxy-fumarate, trans-2,3-Epoxysuccinate, Glycolaldehyde, Ethylene glycol, Formyl-CoA, 3-Oxalomalate, 3-Ethylmalate, 3-Propylmalate, Oxalyl-CoA did not form a metabolic pathway Oxalate does not form a complete metabolic pathway in uv_10, uv_30, and uv_180, and Formyl phosphate does not form a complete metabolic pathway in uv_180, which may be related to the inhibition of related microbial growth or enzyme activity due to excessive UV irradiation. In nitrogen metabolism (map00910), Assimilatory nitrate reduction, Dissimilatory nitrate reduction, Denitrification, and Nitrogen fixation respectively form a complete metabolic pathway, while Nitrification and Anammox do not form a complete metabolic pathway. The relative abundance of Planctomycetes (Vipindas *et al.*, 2020) related to Anammox is only 0.05 to 0.29%, and the corresponding enzymes are 1.7.2.7 and 1.7.2.8, which are both absent in the reaction. The abundance of K20932 and K20935 in the KO database is 0, and the functional genes of Hdh and K20932 are also 0, that is, high altitude environmental factors have a strong inhibitory effect on the functional genes, enzymes, and metabolic pathways related to Anammox. The enzymes related to nitrification are 1.14.18.3, 1.14.99.39 and 1.7.2.6, and the corresponding K10944 and K10535 are almost 0 in the KO database, and the functional genes of pmoA-amoA and hao are almost non-existent. The plateau environment has a strong inhibitory effect on functional genes, enzymes and metabolic pathways related to Nitrification. In turn, the reactions related to Nitrification and Anammox in Plateau environment are inhibited. The sum of the relative abundances of five nitrogen metabolic pathways in five samples is 5.620%, 5.692%, 5.719%, 5.767%, and 5.800%, which means that the relative abundance of nitrogen metabolic pathways is significantly positively correlated with UV radiation ($p<0.05$). The nitrogen metabolism diagram is incomplete in Plateau environment. The abso-lute abundance of nitrogen metabolism pathways under UV rays shows a downward trend. Among the five meta-bolic pathways, the metabolic pathways except Glyoxylate and dicarboxylate metabolism (map00630) are almost the same. UV rays mainly affect the abundance of nitrogen metabolism pathways, and the plateau environment inhibits the structure of the Cyanoamino acid metabolism (map00460) metabolic diagram most severely.

In the phosphorus metabolism pathway, the metabolic diagram formed by Oxidative phosphorylation (map00190) in five samples are completely consistent, but only one of the six NADH dehydrogenases related to ATP, NADH:quinone oxidoreductase, prokaryotes is complete. Among the three Succinate dehydrogenase/Frnarate reductases related to ATP, Succinate dehydrogenase and prokaryotes are complete. Cytochrome bc1 complex respiratory unit is complete in the two Cytochrome reductases related to ATP. Among the four Cytochrome coxidases related to ATP, Cytochrome c oxidase, prokaryotes and Cytochrome o ubiquinol oxidase are complete. In addition, Cytochrome c oxidase, cbb3-type, Cytochrome c, F-type ATPase (Bacteria) and V/A-type ATPase (Bacteria, Archaea) are complete. The oxidative phosphorylation metabolism related to ATP synthesis is relatively simple, and the interaction process with

oxidative phosphorylation in high altitude environment is composed of the above-mentioned relatively single links. The sum of the relative abundances of the two phosphorus metabolism pathways in the five samples were 3.628%, 3.758%, 3.8655%, 3.842%, 3.879%. In Plateau environment, the phosphorus metabolism diagram is incomplete, and the absolute abundance of the phosphorus metabolism pathway under the action of UV rays shows a downward trend. The metabolic pathways in the two metabolic pathways are completely the same, that is, UV rays mainly affects the abundance of the phosphorus metabolism pathway.

4. Discussion

This study reveals the main environmental factors that affect the microbial functional diversity and community structure in wastewater treatment process under UV irradiation. In Plateau environment, NMDS analysis showed that the bacterial community composition of the samples was significantly different ($P<0.001$), and the number of OTUs in the samples increased significantly under UV radiation, that is, UV radiation would increase the types of microorganisms and thus promote the diversity of water treatment system, which may be related to the mutation of OTUs caused by the effect of UV radiation on the genetic recombination of OTUs. The mechanism of action in this regard remains to be revealed by subsequent further studies.

Further analysis of the key species of five samples showed that at the phylum level, the total abundance of the top five key species showed varying degrees of decline under UV irradiation. Among them, UV irradiation can increase the relative abundance of *Bacteroidetes* by 2.32 times, and the strengthening effect is very obvious. It has inhibitory effect on *Proteobacteria* and *Actinobacteria*, which can reduce the relative abundance by 9.58% and 13.00%, respectively. The effect on *Chloroflexi* and *Chlamydiae* depends on the irradiation time, and *Chlamydiae* was first discovered as a key species in Plateau environment. 9 key species were analyzed at the genus level. UV radiation has an intensifying effect on *norank_f__AKYH767*, *norank_f__Saprospiraceae* and *Ottowia*, and has an inhibitory effect on *Acinetobacter*, *IMCC26207*, *Candidatus_Microthrix*, *Gordonia*, and *Comamonas*. The effect on *Trichococcus* depends on the irradiation time. The abundance changes of *Comamonas* have a high consistency with the literature (Zhao *et al.*, 2005), and the key species *norank_f__AKYH767* has not been recorded before, but in view of its highest abundance and strong adaptability, it is urgent to study it later. The above-mentioned species at the phylum and genus levels are key species in Plateau environment, and the difference in their abundance changes is exactly the same as the description that the sensitivity of various bacteria in activated sludge to UV rays is consistent with (Zhao *et al.*, 2007).

According to the analysis of the influence of UV, temperature, DO, pH and water quality on the composition of the water treatment ecosystem, it is found that UV, pH, TN, NH_3-N and COD are all having greater impact on key species at the phylum and genus levels. The driving effect of UV on key species is mainly related to the mutation in OTUs gene recombination. The impact of pH on key species is mainly related to the neutral environment in which they live. The impact of COD on key species mainly related to carbon source competition (Mustakhimov *et al.*, 2013; Wang *et al.*, 2018). The key species affected by TN are nitrogen-fixing and denitrifying bacteria, or denitrifying bacteria, while the key species affected by BOD_5 are mainly due to the consequences of carbon source competition. Obviously, the above-mentioned environmental factors have different reasons for the impact of key species. Key species are highly sensitive to one or several environmental factors, and the selective interference of different environmental factors is also the reason for the diversity of water treatment ecosystems.

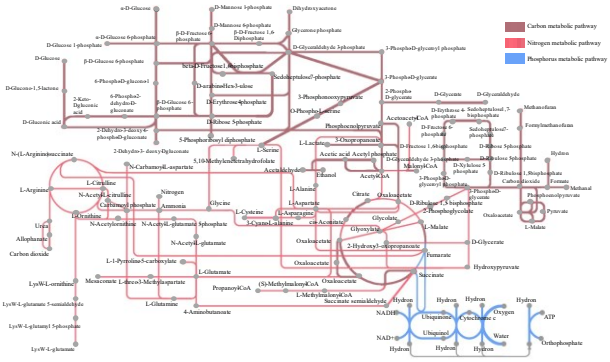

Figure 11. Diagram of carbon, nitrogen and phosphorus metabolism.

The difference analysis of five samples under UV rays shows that each sample has formed three relatively independent network diagrams, whose composition is exactly the same as that of key species. This phenomenon shows that the structure of the water treatment ecosystem is composed of closer microbes, and closer refers to symbiosis or antagonism which is mainly reflected in the competition of the same nutrient source and the interaction of biochemical reactions. It is generally considered to be the result of environmental factors, and the common dominant bacteria show that 33 genera remain unchanged, and the relative abundance of only 17 genera of dominant bacteria will undergo changes in environmental adaptability. So UV radiation can change the composition of the network diagram of closer dominant bacteria.

The analysis of metabolic pathways for five samples showed that UV irradiation will have an intensified or inhibited effect on the top 20 dominant metabolic pathways involved in metabolism. Further research on the metabolism of carbon, nitrogen and phosphorus can reveal that UV radiation can change the relative abundance of metabolic pathways related to carbon, nitrogen and phosphorus. Further metabolic diagram analysis showed that the Arginine biosynthesis (map00220) metabolic diagram in the carbon metabolism diagram is complete and identical, Glycolysis/ Gluconeogenesis (map00010), Carbon fixation in photo-synthetic organisms (map00710), Pentose phosphate

pathway (map00030), Methane metabolism (The metabolic diagram of map00680) is incomplete but it is completely consistent, and the metabolic diagram of Carbon fixation pathways in prokaryotes (map00720) is incomplete and not completely consistent.

The metabolic diagram of Arginine biosynthesis (map00220) in nitrogen metabolism in the five samples are complete and identical, and the metabolic diagram of Alanine, aspartate and glutamate metabolism (map00250), Cyanoamino acid metabolism (map00460), and Nitrogen metabolism (map00910) are incomplete but identical. The metabolism diagram of Glyoxylate and dicarboxylate metabolism (map00630) is incomplete and different. Among them, Nitrogen metabolism (map00910) only has ssimilatory nitrate reduction, Nitrogen fixation, Dissimilatory nitrate reduction, and Denitrification in the metabolic diagram. Nitrification and Anammox are missing. The plateau environment has a strong inhibitory effect on the functional genes, enzymes, and metabolic pathways related to the two metabolisms of Nitrification and Anammox, causing the part of the nitrogen metabolism diagram to be missing. The absence of Anammox will prevent ammonia from being oxidized to nitrite or nitrate in an anaerobic state (Pan *et al.*, 2021), and the removal efficiency of ammonia will decrease. The lack of Nitrification will cause obstacles in the conversion of ammonia to nitrate or nitrite (Tang *et al.*, 2020). The Cyanoamino acid metabolism (map00460) metabolism diagram caused by the plateau environment is more severely missing. The above reasons are the reasons for the poor denitrification effect in Plateau environment. The metabolic diagram of Oxidative phosphorylation (map00190) and Pentose phosphate pathway (map00030) involved in the phosphorus metabolism pathway are exactly the same, but their corresponding metabolic diagram are incomplete and the metabolic links are too single, which is also the reason that restricts the effect of plateau phosphorus removal. The reason for the above metabolic diagram may be related to the influence of the plateau environment on the corresponding metabolic pathways and activated enzymes, and the specific driving mechanism are yet to be revealed by subsequent studies. The relative abundance of carbon, nitrogen and phosphorus metabolic pathways increases under UV radiation, while the absolute abundance appears to decrease. At the same time, the plateau environment also has a certain inhibitory effect on the integrity of most metabolic pathways. The plateau environment affects the composition of the metabolic diagram, and UV radiation only affects the abundance of metabolic pathways.

5. Conclusions

UV radiation showed obvious differences in the bacterial communities of the samples. The bacterial diversity had a great difference in the responsiveness of the driving factors. The most influential driving factors are UV, COD, pH, TN and NH_3-N. The bacterial communities in the five samples show different environmental preferences and environmental vulnerabilities. Further network co-occurrence analysis shows that the structure of the water treatment ecosystem is composed of closer microorganisms, which is mainly reflected in the mutual promotion of nutrition source competition and biochemical reactions as well as environmental adaptability. The carbon, nitrogen, and phosphorus metabolic pathways carried out found that the abundance of metabolic pathways in Plateau environment has a certain change, and the metabolic diagram is almost identical. UV radiation mainly affects the abundance of metabolic pathways, and the plateau environment has a decisive effect on the composition of the metabolic diagram. The plateau environment and UV radiation as important influencing factors have a certain impact on the microbial structure and metabolic pathways, and the further impact mechanism remains to be further revealed in the later period.

Acknowledgments

This work was supported by the National Natural Science Foundation of China (NO. 51868069, 51769034), Natural Science Foundation of Tibet (NO. XZ 2018 ZR G-20), the Program for Scientific Research Innovation Team in Colleges and Universities of Tibet Autonomous Region.

References

Callahan B.J., McMurdie P.J., Rosen M.J., Han A.W., Johnson A.J.A., and Holmes S.P. (2016). DADA2: High-resolution sample inference from Illumina amplicon data. *Nature methods*, ***13***(7), 581–583. https://doi.org/10.1038/nmeth.3869

Dewen L., Ying L., Dandan D., Yuangang Z., Zhonghua T., and Yusen Z. (2020). Analysis of Leaf Trait and Differentially Expressed Genes of Leaf Development in Eucommia ulmoides Oliver after Ultraviolet-B (UV-B) Radiation. https://doi.org/10.21203/rs.3.rs-97641/v1

Gao H.j., Wang B.S., Wang Y., and Zhang Z.X. (2020). Electric Field Stress on Microorganisms in Biofilm Diversity Impact Study. *Green Science and Technology*, 02, 132–138. https://doi.org/10.16663/j.cnki.lskj.2020.02.045. (in Chinese)

Gelsor N., Ya-ming J., Wangmu T., Yi Z., Balma S., and Tunzhu D. (2019). Ground-based measurements of global solar radiation and UV radition in Tibet. *Spectroscopy and Spectral Analysis*, ***39***(6), 1683–1688. https://doi.org/10.3964/j.issn.1000-0593(2019)06-1683-06.

Hao K.Y., Li Y.W., Zong Y.C., You J.H., and Guo M.Z. (2021). Microbial mechanism of A^2O process for wastewater treatment in plateau habitat. *China Environmental Science*, ***41***(05), 2240–2251. https://doi.org/10.19674/j.cnki.issn1000-6923.2021.0236. (in Chinese)

Hao K.Y., Zhang N., Li Y.W., and Zong Y.C. (2021). Effect of ultraviolet radiation on nitrogen and phosphorus removal from sewage in plateau environment. *Desalination and Water Treatment*, ***216***, 232–238. https://doi.org/10.5004/dwt.2021.26866

Hou J.W., Xing C.F., Deng X.M., and Chen F. (2020). Effect of pH on soil bacterial community s structure in root zone of prickly ash. *Journal of Northwest A & F University (Natural Science Edition)*, ***48***(05), 115–122. https://doi.org/10.13207/j.cnki.jnwafu.2020.05.014 (in Chinese).

Hughes K.A. (2005). Effect of Antarctic solar radiation on sewage bacteria viability. *Water Research*, ***39***(11), 2237–2244. https://doi.org/10.1016/j.watres.2005.04.011

Jiang Y X., Sun P S., Liu A W., Li W M., He S X. (2003). Enhancement of phosphorus removal property of activated sludge with UV ray irradiation. *China Environmental Science*, 2003, **23**(2), 184–188. https://doi.org/CNKI:SUN:ZGHJ.0.2003-02-018 (in Chinese).

Li L., Yue C.L., Zhang H., Li H.P., Yang L., and Wang J. (2019). Correlation Between Water Purification Capacity and Bacterial Community Composition of Different Submerged Macrophytes. *Environmental Science*, ***40***(11), 4962–4970. https://doi.org/10.13227/j.hjkx.201903265. (in Chinese).

Merzouki M., Delgenes J.P., Bernet N., Moletta R., and Benlemlih M. (1999). Polyphosphate-accumulating and denitrifying bacteria isolated from anaerobic-anoxic and anaerobic-aerobic sequencing batch reactors. *Current microbiology*, **38**(1), 9–17.

Monyethabeng M.M., and Krügel M. (2016). The effect of UV-C treatment on various spoilage microorganisms inoculated into Rooibos iced tea. *Lwt*, ***73***, 419–424. https://doi.org//10.1016/j.lwt.2016.06.045

Mustakhimov I., Kalyuzhnaya M.G., Lidstrom M.E., and Chistoserdova L. (2013). Insights into denitrification in Methylotenera mobilis from denitrification pathway and methanol metabolism mutants. *Journal of bacteriology*, ***195***(10), 2207–2211. https://doi.org/10.1128/JB.00069-13

Pan J., Huo T., Yang H., Li Z., Chen L., Niu Z., and Liu S. (2021). Metabolic patterns reveal enhanced anammox activity at low nitrogen conditions in the integrated I-ABR. *Water Environment Research*, ***93***(8), 1455–1465. https://doi.org/10.1002/wer.1511

Peng T., Feng C., Hu W., Chen N., He Q., Dong S., and Li M. (2018). Treatment of nitrate-contaminated groundwater by heterotrophic denitrification coupled with electro-autotrophic denitrifying packed bed reactor. *Biochemical Engineering Journal*, **134**, 12–21.

Quast C., Pruesse E., Yilmaz P., Gerken J., Schweer T., Yarza P., and Glöckner F.O. (2012). The SILVA ribosomal RNA gene database project: improved data processing and web-based tools. *Nucleic acids research*, ***41***(D1), D590–D596. https://doi.org/10.1093/nar/gks1219

Tang L., and Deshusses M.A. (2020). Novel integrated biotrickling filter–anammox bioreactor system for the complete treatment of ammonia in air with nitrification and denitrification. *Environmental Science and Technology*, ***54***(19), 12654–12661. https://doi.org/10.1021/acs.est.0c03332

Vipindas P.V., Krishnan K.P., Rehitha T.V., Jabir T., and Dinesh S.L. (2020). Diversity of sediment associated Planctomycetes and its related phyla with special reference to anammox bacterial community in a high Arctic fjord. *World Journal of Microbiology and Biotechnology*, ***36***(7), 1–15. https://doi.org/10.1007/s11274-020-02886-3

Wang B., Zhao M., Guo Y., Peng Y., and Yuan Y. (2018). Long-term partial nitritation and microbial characteristics in treating low C/N ratio domestic wastewater. Environmental Science: *Water Research and Technology*, **4**(6), 820–827.

Wang Y., Gong B., Lin Z., Wang J., Zhang J., and Zhou J. (2018). Robustness and microbial consortia succession of simultaneous partial nitrification, ANAMMOX and denitrification (SNAD) process for mature landfill leachate treatment under low temperature. *Biochemical Engineering Journal*, ***132***, 112–121. https://doi.org/10.1016/j.bej.2018.01.009

Wei W. (2012). Effect of Ultraviolet Radiation on Nitrogen and Phosphorus Removal of Activated Sludge. *Hubei Paper*, (1), 19–24. https://doi.org/CNKI:SUN:FBZZ.0.2012-01-007 (in Chinese)

Wu Y., Shukal S., Mukherjee M., and Cao B. (2015). Involvement in denitrification is beneficial to the biofilm lifestyle of Comamonas testosteroni: a mechanistic study and its environmental implications. *Environmental Science and Technology*, **49**(19), 11551–11559.

Xia Y., Wen X., Zhang B., and Yang Y. (2018). Diversity and assembly patterns of activated sludge microbial communities: a review. *Biotechnology Advances*, ***36***(4), 1038–1047. https://doi.org/10.1016/j.biotechadv.2018.03.005

Xian W.D., Zhang X.T., and Li W.J. (2020). Research status and prospect on bacterial phylum Chloroflexi. *Acta Microbiologica Sinica*, 60(9):1801-1820. https://doi.org/10.13343/j.cnki.wsxb.20200463. (in Chinese)

Yan J.L. (2015). Isolation, Characterization and Gene Function of Highly Efficient DEHP-degrading Bacteria. *Central China Normal University*, https://kns.cnki.net/KCMS/detail/detail.aspx?dbname=CMFD201702&filename=1015442831.nh (in Chinese)

Yang C., Sun W., and Ao X. (2020). Bacterial inactivation, DNA damage, and faster ATP degradation induced by ultraviolet disinfection. *Frontiers of Environmental Science and Engineering*, ***14***(1), 1–10. https://doi.org/10.1007/s11783-019-1192-6

You J H., Zong Y C., Wang J *et al.* (2022). Effect of hydraulic retention time on Microbial Community Structure and Nitrogen Metabolism in anaerobic-anoxic-oxic. *Desalination and Water Treatment*, **259**, 54–63.

Yuanwei L., Hao K., Guo M., You J., and Zong Y. (2021). Characteristics of the community-structure of A2O processes under different dissolved oxygen conditions in plateau areas. In *IOP Conference Series: Earth and Environmental Science,* **657**(1), 012030. IOP Publishing. https://doi.org/10.1088/1755-1315/657/1/012030

Zhang L., Delgado-Baquerizo M., Shi Y., Liu X., Yang Y., and Chu H. (2021). Co-existing water and sediment bacteria are driven by contrasting environmental factors across glacier-fed aquatic systems. *Water Research*, ***198***, 117139. https://doi.org/10.1016/j.watres.2021.117139

Zhao X., Wang Z., Wu Z., Chen L and Zhang F. (2007). Microbial survival rates in UV-irradiated activated sludge. *Acta Scientiae Circumstantiae*, ***27***(7), 1163–1167. https://doi.org/10.13671/j.hjkxxb.2007.07.015 (in Chinese).

Zhao X.F. (2005). Influence of low energy N+ and UV on the structure of Microbial community in activated sludge. *Zhengzhou University*. https://doi.org//kns.cnki.net/KCMS/detail/detail.aspx?dbname=CMFD0506&filename=2005138963.nh (in Chinese).

Zhou D., Zhang Q., Li P., Pan L., and Tu K. (2020). Combined transcriptomics and proteomics analysis provides insight into metabolisms of sugars, organic acids and phenols in UV-C treated peaches during storage. *Plant Physiology and Biochemistry*, ***157***, 148–159. https://doi.org//10.1016/j.plaphy.2020.10.022

Zong Y C. (2017). Preliminary Influence Study of Tibet Natural Environment on Sewage Treatment Effect. *Municipal Engineering Technology*, ***35***(03), 132–135. https://doi.org/CNKI:SUN:SZJI.0.2017-03-048 (in Chinese).

Zong Y.C., Hao K.Y., Li Y.W., Lu G.H., and Huang D.C. (2019). Nitrogen and phosphorous removal of pilot-scale anaerobic-anoxic-aerobic process under plateau environmental factors. *Applied Ecology and Environmental Research*, ***17***(5), 12213–12226. https://doi.org/10.15666/aeer/1705_1221312226

Zong Y., Li Y., Hao K., Lu G., and Huang D. (2019). Influence of transient change of water temperature on pilot-scale anaerobic-anoxic-oxic process under plateau environmental factors. *J. Applied Ecology And Environmental Research*, ***17***, 12191–12202. http://dx.doi.org/10.15666/aeer/1705_12191 12202

ZongY., Li Y., Huang D., Hao K., and Lu G. (2020). Characteristics of the community-structure of A2O processes under different temperature conditions in plateau areas. *Applied Ecology and Environmental Research*, ***17***(2), 5081–5091. https://doi.org/10.21203/rs.3.rs-45362/v1

Zong Y.C., Zhang Y.H., Lu G.H., and Chen X.Y. (2018). Study on process characteristics of high altitude A2/O process based on principal component analysis, Technol. *Water Treatment*, **44,** 116–119. (in Chinese)